EXPERIMENTAL METHODS AND PROCESSING OF DATA

ACTIVATION OF ^{93}Nb NUCLEI ON THE LINAC LUE-40 OF RDC "ACCELERATOR" AND DETERMINATION OF PHOTONUCLEAR REACTION CROSS-SECTIONS

O.M. Vodin, O.S. Deiev, S.M. Olejnik

National Science Center "Kharkov Institute of Physics and Technology", Kharkiv, Ukraine
E-mail: deev@kipt.kharkov.ua

The bremsstrahlung spectra of medium-energy electrons (30…100 MeV) were calculated in *GEANT4*. Cross-sections for photonuclear reactions were calculated in *TALYS1.9*. A convolution over the energy of the cross-sections of one- and many-particle reactions with the bremsstrahlung flux density was performed. The numerical values of the yield of ^{93}Nb$(\gamma,xn)^{93-x}$Nb reactions, the activity of irradiated ^{93}Nb targets, and the average reaction cross-sections were obtained. The differences of the bremsstrahlung spectra from electrons with close initial energies were calculated. The shape of the difference spectra was analyzed. The contributions of the quanta of the low-energy part of the difference spectrum and the quasi-monochromatic peak of the difference spectrum to the total activity of the targets were compared. An approach for correction of the experimental cross-sections of photonuclear reactions using the method of "bremsstrahlung spectra difference" was considered.

PACS: 07.85.Fv, 61.80.Cb

INTRODUCTION

The bremsstrahlung γ-radiation of electrons from converter-target is an important nuclear-physical instrument of modern nuclear physics and used in various applications. It is necessary to correctly calculate the spectral-angular characteristics of γ-radiation, numerically evaluate the flux of radiation incident on the target. Such calculations are important in the production of isotopes or activation of target atoms using photonuclear reactions. The calculation of bremsstrahlung and the yields of nuclear reaction products are important when using power plants based on subcritical systems controlled by an electronic accelerator.

The calculation method of bremsstrahlung spectra is well known. In the case of thin targets, the spectrum is described analytically by the Schiff formula [1], but in the case of thick targets, this formula is not applicable. For real experimental measurements, the certified open-source code *GEANT4* is widely used [2]. The *GEANT4* program code, *PhysListLowEnergy*, allows one to calculate the bremsstrahlung spectra with all physical processes for the case of an amorphous target [3, 4]. Similarly, *PhysList QGSP BIC HP* makes it possible to calculate the neutron yield due to photo-nuclear reactions from targets of various thicknesses and atomic charges [4].

The objectives of this work are:

− simulation in *GEANT4* of the spectral-angular distributions of the bremsstrahlung γ-radiation of medium-energy electrons from an amorphous Ta-converter target, taking into account the passage of radiation through an Al-absorber;

− estimation of the yield of electrons and photoneutrons from converters and absorbers;

− calculation of cross-sections for ^{93}Nb$(\gamma,xn)^{93-x}$Nb in *TALYS1.9* [5];

− obtaining the numerical value of the reaction yield, the activity of the irradiated ^{93}Nb targets, estimating the average value of the reaction cross-section;

− calculate the bremsstrahlung difference spectra, examine an approach for adjusting the experimental cross-sections of photonuclear reactions, and obtain numerical values of the cross-sections using the "difference of γ-quanta" method.

1. CALCULATION BREMSSTRAHLUNG RADIATION SPECTRA AND DIFFERENCES OF GAMMA-QUANTA SPECTRA IN GEANT4

The bremsstrahlung spectra of medium-energy electrons (30...100 MeV) were calculated in *GEANT4*. The calculations used the real geometry of the experiment, taking into account the spatial and energy spread of the electron beam. The axis of the electron beam corresponds to the 0 angles.

Typical conditions for calculations and experiment: the thickness of the Ta-converter is l(Ta) = 1.05 mm, the distance between the Ta-converter and the ^{93}Nb target was D = 248 mm. Target radius R_{targ} = 4 mm. The radius of the electron beam is R_e = 2.5 mm. The energy spread of the electron beam is $FWHM$ = 2.35% of E_e. In the Fig. 1,a,b shows the bremsstrahlung spectra for an Al-absorber l(Al) = 0 and 150 mm. Fig. 2,a,b shows the corresponding spectra of the γ-quanta difference for two close energies of incident electrons.
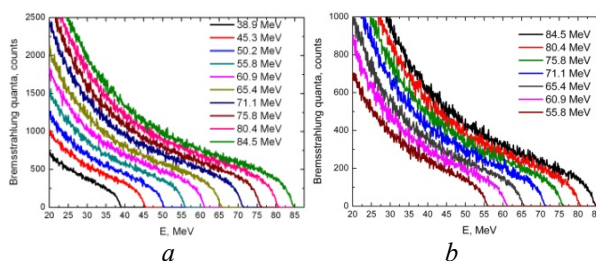

Fig. 1. γ-Spectra for various E_e, l(Al) = 0 mm (a); γ-Spectra for various E_e, l(Al) = 150 mm (b)

The number of quanta in the energy range E_e = 30...100 MeV proportionally increases with increasing electron energy. The peaks of the difference spectra are distinguished, but there is also a low-energy part of the difference spectrum. The number of quanta

in the low-energy part of the spectrum in total exceeds the sum of the quanta in the quasi-monochromatic peak of the difference spectrum. Thus, to call such a difference spectrum quasi-monochromatic is incorrect.
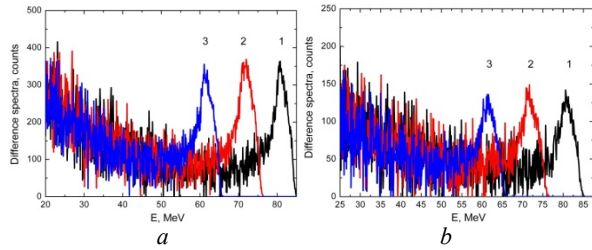

Fig. 2. Spectra of the γ-quanta difference, l(Al) = 0.
1 – 84.4...80.4 MeV; 2 – 75.8...71.1 MeV;
3 – 65.4...60.9 MeV (a); spectra of the γ-quanta
difference, l(Al) = 150 mm. 1 – 84.4...80.4 MeV;
2 – 75.8...71.1 MeV; 3 – 65.4...60.9 MeV (b)

The number of quanta in the energy range E_e = 30...100 MeV proportionally increases with increasing electron energy. The peaks of the difference spectra are distinguished, but there is also a low-energy part of the difference spectrum. The number of quanta in the low-energy part of the spectrum in total exceeds the sum of the quanta in the quasi-monochromatic peak of the difference spectrum. Thus, to call such a difference spectrum quasi-monochromatic is incorrect.

The total number of quanta in the calculated spectra (E_γ = 38.9...84.5 MeV) when using a l(Al) = 150 mm Al-absorber is 0.59...0.64, and for 100 mm is 0.44...0.48 of the total quanta in the absorber absence. The shape of the spectrum of the γ-quanta difference deteriorates in the presence of an absorber. This refers to a decrease in the ratio of the peak area to the total area of the difference spectrum by about 25...30%.

2. CALCULATION OF THE CROSS-SECTION OF PHOTONUCLEAR REACTIONS ^{93}Nb(γ,xn)$^{93-x}$Nb IN TALYS 1.9

Calculations of the cross-section of photonuclear reactions ^{93}Nb(γ,xn)$^{93-x}$Nb were performed in *TALYS1.9* [8].
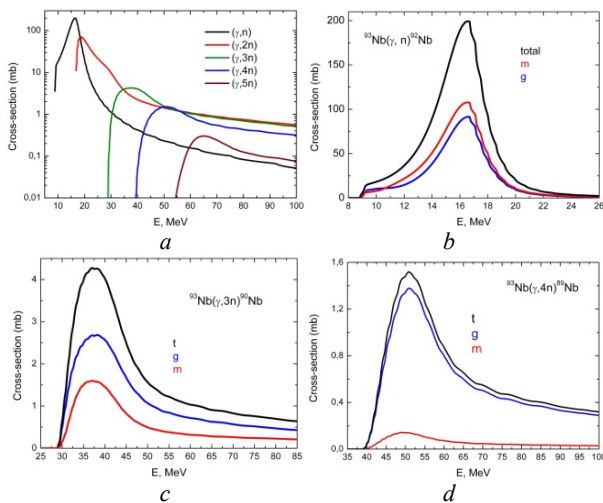

Fig. 3. ^{93}Nb(γ,xn)$^{93-x}$Nb total cross-sections (a);
^{93}Nb(γ,n)^{92}Nb cross-sections (b); ^{93}Nb(γ,3n)^{90}Nb
cross-sections (c); ^{93}Nb(γ,4n)^{89}Nb cross-sections (d)

Fig. 3,a,b,c,d shows some calculated cross sections in the energy range up to 100 MeV, where g – for the ground

state, m – for the metastable state, and $t = (m+g)$ – total cross section. These cross-sections were used in the calculation of the convolution of cross-sections with a bremsstrahlung flux to obtain the reaction yield, averaged cross-sections, as well as for comparison with experimental data.

3. BREMSSTRAHLUNG AND ELECTRONS SPECTRA PASSING THROUGH A TARGET. THE ROLE OF THE ABSORBER

The calculation of the bremsstrahlung spectra in *GEANT4* for E_e = 84.5 MeV are presented in Fig. 4. Also shown the electrons spectra and the total reaction cross-sections for ^{93}Nb(γ,xn)$^{93-x}$Nb. Convolutions with all cross-sections with the γ-quanta and electrons flux corrected for the fine structure constant 1/137 were performed. The yields of the reactions Y_γ and Y_e/137 were determined.
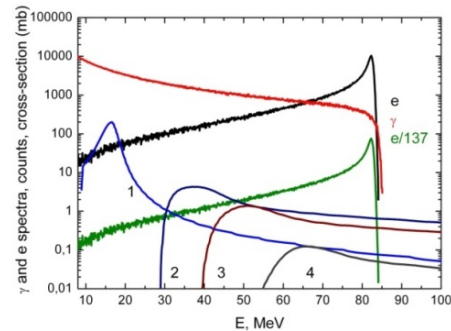

Fig. 4. The calculated γ-quanta and electron spectra
without an absorber. E_e = 84.5 MeV, Ta = 1.05 mm,
D = 248 mm. Cross-section of photonuclear reactions
^{93}Nb(γ,xn)$^{93-x}$Nb

The ratio of the reaction yields for γ-quanta to the reaction yields for electrons Y_γ/(Y_e/137) was 12536 for ^{93}Nb(γ,n)^{92}Nb, 328 for ^{93}Nb(γ,3n)^{90}Nb, 153 for ^{93}Nb(γ,4n)^{89}Nb, 67 for ^{93}Nb(γ,5n)^{88}Nb. E_e = 84.5 MeV. For E_e = 38.9 MeV the ratio Y_γ/(Y_e/137) was 1887 for ^{93}Nb(γ,n)^{92}Nb, 32 for ^{93}Nb(γ,3n)^{90}Nb.

Therefore, the contribution of γ-quanta to the reaction yield dominates for all reactions and all experimental energies in the absence of an absorber. Thus, the use of an aluminum absorber is advisable mainly to relieve heat and radiation load on the target and structural elements.

In [6], W with a thickness of 100 µm was used to generate bremsstrahlung. Absorber and electron turning were not used. We calculated the contribution of electrons to photonuclear reactions for E_e = 70 MeV. The ratio of the reaction yields Y_γ/(Y_e/137) was 1815 for ^{93}Nb(γ,n)^{92}Nb, 9.8 for ^{93}Nb(γ,n)^{92}Nb, 3.9 for ^{93}Nb(γ,4n)^{89}Nb, 0.67 for ^{93}Nb(γ,5n)^{88}Nb. The contribution of γ-quanta to the reaction yield dominates for all reactions, except ^{93}Nb(γ,5n)^{88}Nb, where the contribution of electrons is greater than the contribution of γ-quanta.

In experiments, it is necessary to find a balance between the good shape of the bremsstrahlung spectra and the removal of the electronic component responsible for heating the target. Calculations showing changes in bremsstrahlung and electronic spectra with an Al - absorber of l(Al) = 0 and 100 mm were performed.

For bremsstrahlung, in the presence of an absorber, the spectrum retains its shape, while the number of

quanta decreases to ~ 2 times. The electrons spectrum in the presence of an absorber completely changes. Almost complete electrons absorption was observed. The total electrons number is less than the γ-quanta number by 20…30 times for various initial energies of E_e. Also, the electron energy is greatly reduced. The radiation load on the target decreases strongly.

In the experiment with an absorber, there are significant minuses: deterioration in the shape of the bremsstrahlung spectra difference and an additional generation of neutrons. In *GEANT4* the calculations the neutron flux in a full solid angle of 4π were performed. The ratio of the neutrons yields Y_n. $Y_n(l(Ta) = 1 \text{ mm})/Y_n(l(Al) = 100 \text{ mm})/Y_n(l(Ta) = 1 \text{ mm} + l(Al) = 100 \text{ mm})$ was $(0.02/0.24/0.33)$ n/s/kW/10^{12}. Most neutrons are generated in an Al-absorber. The number of emitted neutrons $Y_n(l(Ta) = 1 \text{ mm} + l(Al) = 100 \text{ mm})$ was $4 \times 10^{10} \ldots 1.3 \times 10^{11}$ n/s, for $E_e = 40 \ldots 100$ MeV and $I_e = 4$ μA.

4. DEPENDENCE OF THE BREMSSTRAHLUNG FLUX ON THE TARGETS POSITION AND THE SIZE

4.1. DEPENDENCE OF THE BREMSSTRAHLUNG FLUX ON THE TARGET SIZE

In activation experiments, the target area should be completely covered by high-energy bremsstrahlung quanta. This is necessary to accurately assess the number of atoms in the target that are involved in activation. It is necessary to estimate the maximum radius of the target where such a requirement is reliably fulfilled.

In *GEANT4* the bremsstrahlung spectra were calculated as a function of the target radius R. Dependency estimates were performed in two ways. In the first approach, the dependence of the total bremsstrahlung flux of different energy ranges on the target radius $N_\gamma(R)$ was studied. This dependence has an increasing character and it is convenient to normalize it to a target of infinite radius. The dependences of the bremsstrahlung yield $N_\gamma(R)$ on the target radius are shown in Fig. 5,a ($E_e = 100$ MeV, $l(Ta) = 1$ mm, $l(Al) = 0$, $D = 250$ mm). In this geometry, a saturation of the yield does not occur for all energy ranges up to $R \sim 20$ mm.

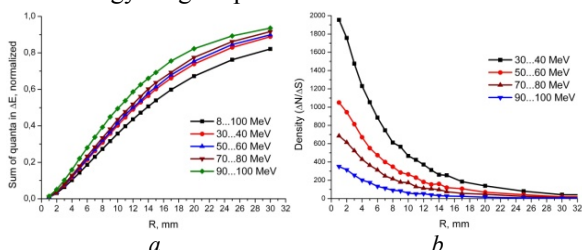*a*   *b*

Fig. 5. Dependence of the bremsstrahlung flux $N_\gamma(R)$ on R (a); dependence of densities of bremsstrahlung flux $\Delta N_\gamma(R) / \Delta S(R)$ on R (b)

In the second approach, the densities of bremsstrahlung radiation yield were calculated: $\Delta N_\gamma(R)$ divided by $\Delta S(R)$. $\Delta S(R)$ is the area of the ring formed by the difference of two target circles. $\Delta N_\gamma(R)$ − number of quanta falling in $\Delta S(R)$. This dependence decreases with an increasing radius of the target R (Fig. 5,b). Maximum limits on the size of the target appear at $E_e \sim 100$ MeV. In our case, at size up to $R = 10$ mm, the bremsstrahlung flux

reliably completely covers the target. The value $R = 10$ mm is the ultimate target size due to the diameter of the pneumatic line.

Similar dependences of the output of the bremsstrahlung radiation $N_\gamma(R)$ were calculated for electrons with $E_e = 40...90$ MeV. These dependencies are somewhat wider than for electrons with $E_e = 100$ MeV.

A similar calculation was performed for $l(Al) = 100$ and 150 mm. Estimates show a slight decrease in the flux in value and a widening of the dependences of the bremsstrahlung yield on the radius of the target in the presence of an absorber. Thus, with a target size of up to $R = 10$ mm, the quantum flux completely cover the target for all experimental conditions.

4.2. DEPENDENCE OF THE BREMSSTRAHLUNG FLUX ON THE DISPLACEMENT OF THE TARGET CENTER

The displacement of the center of the target relative to the axis of the electron beam is one of the possible experimental errors. It is necessary to evaluate the possible error in the value of the bremsstrahlung flux and, accordingly, the target's activity.

Bremsstrahlung flux was calculated for different displacements of the target center were calculated. It is more convenient to present the results in a normalized form, where the flow for an unbiased target is taken as 1. In Fig. 6,a,b normalized values of bremsstrahlung flux in the energy range $\Delta E = 8…100$ MeV and $\Delta E = 80…100$ MeV are presented for $E_e = 100$ MeV, $l(Ta) = 1$ mm, $R_{targ} = 5$ mm, $R_e = 5$ mm, $D = 100$ and 250 mm, $l(Al) = 0$.
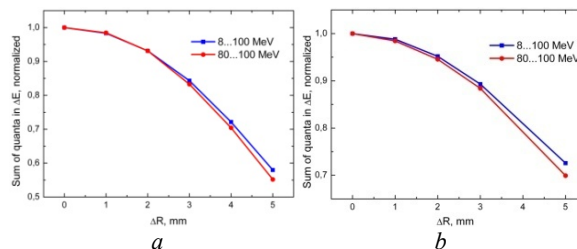

a   *b*

Fig. 6. Normalized bremsstrahlung flux as a function of displacement ΔR. D = 100 mm (a); normalized bremsstrahlung flux as a function of displacement ΔR. D = 250 mm (b)

As the distance between the converter and the target increases, as in the case of a target with a larger radius, the effect of the center displacement somewhat decreases. The Table 1 shows the results of the normalized bremsstrahlung flux for real experiment geometry $E_e = 84.5$ MeV, $l(Ta) = 1.05$ mm, $R_{targ} = 4$ mm, $D = 248$ mm, $l(Al) = 150$ mm.

Table 1

Normalized bremsstrahlung flux, ΔR displacement

ΔR, mm	$\Delta E = 8…84.5$ MeV	$\Delta E = 76…84.5$ MeV
0	1	1
1	0.991	0.975
2	0.957	0.921
3	0.905	0.836

Thus, the experimental error becomes significant even for the displacements of the center of the target of comparable or greater than 2 mm.

4.3. DEPENDENCE THE BREMSSTRAHLUNG FLUX ON DISTANCE CONVERTER-TARGET

The dependence of the bremsstrahlung flux on the distance between the target and the converter was estimated. The calculation of the bremsstrahlung spectra was performed for E_e = 100 MeV, l(Ta) = 1 mm, R_e= 5 mm, R_{targ} = 5 mm. Distance D changed. If the bremsstrahlung flux at D = 100 mm is taken as 1, then at D = 500 mm the attenuation of the flux is about 9 times, at D = 1000 mm, attenuation is 30 times, at D = 2000 mm, attenuation is 100 times. The calculation showed a strong attenuation of the flux of quanta with increasing distance. The dependence of flow on distance does not correspond to a simple dependence as the square of the distance.

5. YIELD AND CROSS-SECTIONS OF ^{93}Nb(g,xn)$^{93-x}$Nb REACTIONS
5.1. ESTIMATED YIELD OF ONE- AND MULTI-PARTICLE REACTIONS IN *GEANT4, TALYS1.9*

The convolution over the cross-section energy of the reaction ^{93}Nb(γ,n)^{92}Nb and ^{93}Nb(γ,3n)^{90}Nb (*TALYS1.9*) with bremsstrahlung spectra was performed. This corresponds to the yield of the reaction. The calculation results for the experimental conditions l(Ta) = 1.05 mm, R_{targ} = 4 mm, D = 248 mm are shown in Fig. 7,a,b. For comparison, the results for l(Al) = 0, 100, 150 mm are shown.
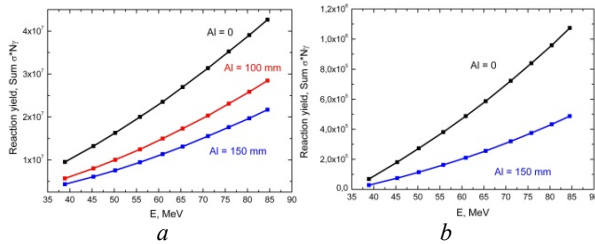

a *b*

Fig. 7. The reaction yield ^{93}Nb(γ,n)^{92t}Nb. l(Al) = 0, 100, 150 mm (a); the reaction yield ^{93}Nb(γ,3n)^{90t}Nb. l(Al) = 0, 150 mm (b)

We note an approximately twofold decrease in the reaction yield when using an l(Al) = 150 mm absorber. Similar dependences of the reaction yield on the energy of incident electrons are calculated for various reactions ^{93}Nb(γ,xn)$^{93-x}$Nb. Dependencies have a smooth growth with increasing energy.

5.2. NORMALIZED VALUES OF EXPERIMENTAL AND CALCULATED REACTION YIELDS

Fig. 8,a,b compares the normalized experimental yields of the ^{93}Nb(γ,n)^{92m}Nb and ^{93}Nb(γ,3n)^{90t}Nb reactions and the calculated yields obtained using *GEANT4* and *TALYS1.9*. In both cases, the yields were normalized to the yield at the maximum experimental energy of 84.5 MeV.

In Fig. 8,a the first three points were measured and counted using the l(Al) = 100 mm converter, the rest with l(Al) = 150 mm. A characteristic change in the reaction yield tendency is connected with this fact. We note some discrepancies between the calculation and the experiment for the ^{93}Nb(γ,n)^{92m}Nb reaction, which is within the experimental error. Similarly, the yields of

the ^{93}Nb(γ,4n)^{89}Nb total, m, g reactions were compared. The agreement of calculations and measurements is satisfactory.
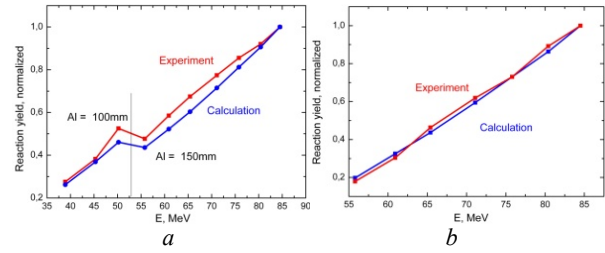

a *b*

Fig. 8. Normalized values of experimental and calculated yields of ^{93}Nb(γ,n)^{92m}Nb (a); normalized values of experimental and calculated yields of ^{93}Nb(γ,3n)^{90}Nb (b)

5.3. CALCULATION OF ENERGY-AVERAGED CROSS-SECTIONS

The calculation of the average energy cross-section $\langle\sigma(E)\rangle$ in a given energy interval was performed according to the formula:

$$\langle\sigma(E)\rangle = \sum(\sigma(E)\times W(E))\Big/\sum W(E), \quad (1)$$

where $\sigma(E)$ − reaction cross-section, $\sum W(E)$ − bremsstrahlung flux density incident on the target. The summation is performedt in the energy interval of averaging the cross-section from the reaction threshold to the maximum energy value E_e.

The average values of the cross-sections obtained using *TALYS1.9* cross-sections and the calculated bremsstrahlung spectra from *GEANT4* are shown in Figs. 9-12.
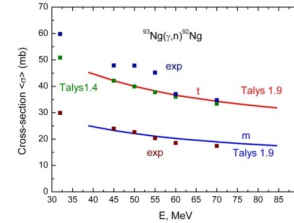

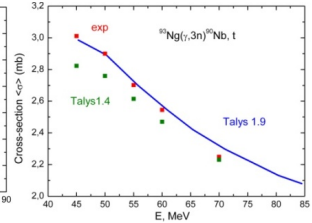*Fig. 9. Averaged cross-sections ^{93}Nb(γ,n)^{92m,t}Nb*

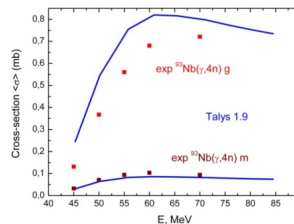

Fig. 10. Averaged cross-sections ^{93}Nb(γ,3n)^{90t}Nb

Fig. 11. Averaged cross-sections ^{93}Nb(γ,4n)^{89g,m}Nb

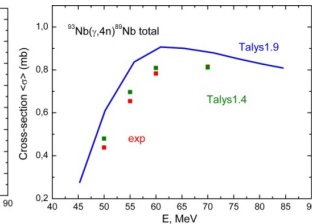*Fig. 12. Averaged cross-sections ^{93}Nb(γ,4n)^{89t}Nb*

The cross-sections are compared with the experimental and calculated results in *TALYS1.4* [6, 7]. Lines − calculations of the present work using *TALYS1.9*. Points − data [6]. Blue lines on Figs. 9-12 − calculations of the present work, points − data [6].

Table 2 shows our calculations (l(Al) = 0) of the relative average reaction cross-sections ^{93}Nb(γ,n)^{92m}Nb, ^{93}Nb(γ,3n)^{90t}Nb, ^{93}Nb(γ,4n)^{89t}Nb for E_e = 65.4, 71.1 and 80.4 MeV. The results are compared with data [6]. Normalized to the cross-section ^{93}Nb(γ,n)^{92m}Nb.

Relative average reaction cross-sections

Reactions	$<\sigma>_{exp}$[6]	$<\sigma>_{cal}$		
$E_{\gamma max}$, MeV	70	65.4	71.1	80.4
$^{93}Nb(\gamma,n)^{92m}Nb$	1	1	1	1
$^{93}Nb(\gamma,3n)^{90t}Nb$	0.129	0.124	0.122	0.119
$^{93}Nb(\gamma,4n)^{89t}Nb$	0.047	0.047	0.047	0.046

Note that there is a 1…2% difference in the mean cross-sections at l(Al) = 0 and 150 mm. This is due to some distortion of the bremsstrahlung spectra during the passage of the absorber.

5.4. CORRECTION OF EXPERIMENTAL CROSS-SECTIONS FOR PHOTONUCLEAR REACTIONS

The quasimonochromatic peak of the difference spectrum can be experimentally shifted in energy from the reaction threshold to the region of high energies (Fig. 13).
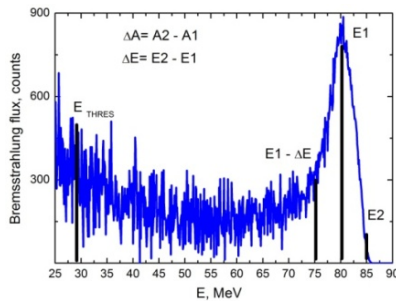

Fig. 13. Bremsstrahlung spectra difference. The lines show E2, E1, E_{THRES}

Under ideal conditions, the low-energy part of the difference spectrum is completely absent. In this case, the difference between the two activities $\Delta A = (A2 - A1)$ was measured at electron energies $E2$ and $E1$ that make up the difference spectrum $(\Delta E = E2 - E1)$. The peak of the difference spectrum is in the range $(E1-\Delta E, E1+\Delta E)$. Next, we calculated $\sum W(E)$ under the peak of the difference spectrum. Then use the formula:

$$\langle \sigma(E) \rangle =$$
$$= \frac{\lambda \Delta A / N_x / I_\gamma / \varepsilon / \sum W(E)}{(1 - exp(-\lambda T_i)) \times exp(-\lambda T_c) \times (1 - exp(-\lambda T_m))}, \quad (2)$$

where N_x is the number of target atoms, $\sum W(E)$ – bremsstraung flux, I_γ the branching intensity of the analyzed γ-rays, ε – the detection efficiency of the activated product, λ is the decay constant ($ln2/T_{1/2}$), T_i, T_c and T_m are the irradiation time, cooling time, measurement time, respectively [6]. In this case, we get the reaction cross-section at a specific point $E1$ of the energy scale, with averaging over the interval ($E1-\Delta E$, $E1+\Delta E$). Advancing the peak in energy, we similarly obtain cross-sections at various energies. As a result, we have the dependence of the reaction cross-section on energy.

Unfortunately, this simple procedure is not applicable in the presence of the low-energy part of the difference spectrum. At each point, a significant contribution of the low-energy part of the difference spectrum to the difference of activities occurs (see Fig. 13). This must be taken into account step by step.

To estimate the average cross-section in the middle of the peak of the difference spectrum, we use the following procedure. It is necessary to estimate the fraction (K) of the peak in the total difference in activities. This value K was obtained by dividing the two yields of the reaction: the yield at the peak of the difference spectrum ($E1-\Delta E$, $E1+\Delta E$) was divided by the yield in the energy range (E_{THRES}-$E2$). The yield for (E_{THRES}-$E2$) is calculated either step by step with the experimental cross-section points or with the cross-section from *TALYS1.9*. Then we calculated the average cross-section at the peak of the difference spectrum. And, respectively, we set the density of the bremsstrahlung flux in the formula (2) in the range of the peak of the difference spectrum – $\sum W(E1 - \Delta E, E1+\Delta E)$. After multiplying the obtained average cross-section by the coefficient K, we obtain an estimate of the cross-section in the interval ($E1-\Delta E$, $E1+\Delta E$) with the average energy in $E1$, which corresponds to the energy difference $\Delta E = E2 - E1$ (see Fig. 13).

This approach was tested by the difference in target witness activity from Mo [8]. The evaluation of the cross-section according to the described procedure was satisfactory. So, for E_e = 70 MeV, the calculation gave 0.13 mb, the cross-section in *TALYS1.9* gives 0.115 mb.

CONCLUSIONS

In this paper, the tasks are set and fulfilled:

− calculation in *GEANT4* was performed of the spectral-angular distributions of the bremsstrahlung γ-radiation of medium-energy electrons from an amorphous Ta-converter target, taking into account the passage of radiation through an Al-absorber;

− cross-sections for photonuclear reactions $^{93}Nb(\gamma,xn)^{93-x}Nb$ in *TALYS1.9* were calculated;

− estimation of the yield of electrons and photoneutrons from converters and absorbers were performed;

− the ratio of the reaction $^{93}Nb(\gamma,xn)^{93-x}Nb$ yields $Y_\gamma/(Y_e/137)$ for γ-quanta to the reaction yields for electrons was obtained;

− numerical values of the yield of $^{93}Nb(\gamma,xn)^{93-x}Nb$ reactions, the activity of irradiated ^{93}Nb targets, and estimates of the average value of the reaction cross-section were obtained;

− the method of "bremsstrahlung spectra difference" was considered, the shape of the spectra difference was shown, the approach for correcting the measured experimental cross-sections was proposed, the numerical values of the cross-sections by this method were obtained.

Data on the cross-sections for photonuclear reactions and the yields of neutron multiplicity in the energy region of incident γ-quanta from 30 to 100 MeV can be used to create power plants based on subcritical systems controlled by an electron accelerator.

REFERENCES

1. L.I. Schiff. Energy-Angle Distribution of Thin Target Bremsstrahlung // *Phys. Rev.* 1951, v. 83, p. 252.
2. Electron and Positron Incident. *http://geant4.web.cern.ch/geant4/*
3. G.L. Bochek, O.S. Deiev, N.I. Maslov. Energy and angular characteristics of electron bremsstrahlung

for different converter // *Problems of Atomic Science and Technology. Series "Nuclear Physics Investigations".* 2012, № 3, p. 223-225.

4. O.S. Deiev, G.L. Bochek, V.N. Dubina, et al. Bremsstrahlung of electrons and yield of neutrons from thick converters, passing of γ-radiation and neutrons through biological shielding // *Problems of Atomic Science and Technology. Series "Nuclear Physics Investigations".* 2019, № 3, p. 65-73.

5. TENDL-2017 Nuclear data library. *http://www.TALYS.eu/home/*

6. H. Naik, G.N. Kim, R. Schwengner, K. Kim, M. Zaman, et al. Photo-neutron reaction cross-section for ^{93}Nb in the end-point bremsstrahlung energies of 12…16 and 45…70 MeV // *Nucl. Phys. A.* 2013, v. 916, p. 168-182.

7. O.M. Vodin, O.A. Bezshyyko, L.O. Golinka-Bezshyyko, et al. Isomer ratios in photonuclear reactions with multiple neutron emission // *Problems of Atomic Science and Technology. Series "Nuclear Physics Investigations".* 2019, № 3, p. 38-46.

8. A.N. Dovbnua, A.S. Deiev, V.A. Kushnir, et al. Experimental results on cross-sections for ^{7}Be photoproduction on ^{12}C, ^{14}N, and ^{16}O nuclei in the energy range of 40…90 MeV // *Phys. of Atomic Nucl.* 2014, v. 77, Issue 7, p. 805-808.

Article received 16.10.2019

АКТИВАЦИЯ ЯДЕР ^{93}Nb НА ЛУЭ-40 НИК «УСКОРИТЕЛЬ» И ОПРЕДЕЛЕНИЕ СЕЧЕНИЯ ФОТОЯДЕРНЫХ РЕАКЦИЙ

А.Н. Водин, А.С. Деев, С.Н. Олейник

Спектры тормозного излучения электронов средних энергий (30…100 МэВ) рассчитывались в *GEANT4*. Сечения фотоядерных реакций рассчитывались в *TALYS1.9*. Проведена свертка по энергии сечений одно- и многочастичных реакций с плотностью потока тормозного излучения. Получены численные значения выхода реакций ^{93}Nb(γ,*x*n)$^{93-x}$Nb, активности облученных мишеней ^{93}Nb, среднее значение сечений реакции. Рассчитаны разности тормозных спектров от электронов с близкими начальными энергиями. Проведен анализ формы спектров разности, выполнено сравнение вкладов в полную активность мишеней, отдельно квантов низкоэнергетической части разностного спектра и квазимонохроматического пика разностного спектра. Рассмотрен подход для корректировки экспериментальных сечений фотоядерных реакций при использовании метода «разности тормозных спектров».

АКТИВАЦІЯ ЯДЕР ^{93}Nb НА ЛУЕ-40 НІК «ПРИСКОРЮВАЧ» І ВИЗНАЧЕННЯ ПЕРЕРІЗУ ФОТОЯДЕРНИХ РЕАКЦІЙ

О.М. Водін, О.С. Деєв, С.М. Олейнік

Спектри гальмівного випромінювання електронів середніх енергій (30...100 МеВ) розраховувалися в *GEANT4*. Перерізи фотоядерних реакцій розраховувалися в *TALYS1.9*. Проведена згортка по енергії перерізів одно- і багаточастинкових реакцій з щільністю потоку гальмівного випромінювання. Отримано чисельні значення виходу реакцій ^{93}Nb(γ,*x*n)$^{93-x}$Nb, активності опромінених мішеней ^{93}Nb, середнє значення перерізів реакції. Розраховано різниці гальмівних спектрів від електронів з близькими початковими енергіями. Проведено аналіз форми спектрів різниці, виконано порівняння вкладів у повну активність мішеней, окремо квантів низькоенергетичної частини різницевого спектра і квазімонохроматичного піку різницевого спектра. Розглянуто підхід для коригування експериментальних перерізів фотоядерних реакцій при використанні методу «різниці гальмівних спектрів».